



Numerical study of CHS-SHS T-joints with chord face failure

Luiza G. V. Alves¹, João B. S. Neto¹, Daniel J. R. Pereira¹, Matheus M. Oliveira¹, Arlene M. C. Sarmanho¹,
Messias J. L. Guerra²

¹*Dept. of Civil Engineering, Federal University of Ouro Preto (UFOP), Morro do Cruzeiro Campus, 35400-000, Ouro Preto - MG, Brazil*

drocha044@gmail.com, matheusmoliveira4@gmail.com, joabatista011@gmail.com,

lluizavasconcellos@gmail.com, arlene@ufop.edu.br

²*Dept. of Civil Engineering, Federal Institute of Minas Gerais (IFMG) – Santa Luiza Campus
junioguerra@hotmail.com*

Abstract. National and international normative prescriptions do not currently predict the design of joints with sections containing high slenderness values. In this work, tubular T-joints containing chords with square hollow sections and braces with circular hollow sections, which offer an easiness to the welding process, were studied with the intention of enabling the of lighter profiles in tubular structures. A numerical model was developed using finite elements in a commercial software (ANSYS), in which the stress distributions, the joint resistance, the failure mode and the load-displacement behaviors were analyzed in joints with different geometric properties. An axial compression load was applied to the brace, and the joint results were compared with the analytical results using the equation recommended by ABNT NBR 16239:2013. Chord face failure was the failure mode found in all profiles analyzed. It was observed that, for higher values of brace diameters and chord thicknesses, higher joint resistance results were found. In the joints analyzed, it was observed that the current normative design equation did not predict the joint resistance values from the numerical model with high accuracy, with a general mean ratio of the normative joint resistance divided by the numerical joint resistance equal to 0.717.

Keywords: Hollow steel sections, T-joints, Chord face failure, Slender sections.

1 Introduction

The use of hollow steel sections is an adequate solution to structures subjected to high levels of axial loads of tension or compression [1]. In Brazil, the current normative prescription – ABNT NBR 16239 [2] – predicts the use of joints between chords and braces composed of hollow steel sections with circular (CHS), rectangular (RHS) or square (SHS) shapes, with limitations in respect to the geometric properties of chords and braces.

The equations used in the design of joints with RHS/SHS chords and CHS braces were obtained from a form factor, which is, therefore, an adaptation from the RHS-RHS joint design equation. Thus, the importance of the development of studies involving tubular CHS-RHS/SHS joints is essential to the understanding of their behavior, especially in cases of joints with geometric properties outside the current normative validity ranges.

Pereira et al. [3] and Neto et al. [4] analyzed, through numerical studies, tubular T-joints with high brace-to-chord ratios and containing chords with sections with high slenderness, which presented chord sidewall failure. It was concluded that the current design equations do not adequately predict the behavior of joints containing chords with slender cross sections. Pereira et al. [5] analyzed CHS-RHS T-joints with chords containing slender sections, and observed that the same failure mode – chord face failure – present in joints inside the normative validity ranges was observed in the joints analyzed, which were outside these validity ranges.

In this context, this work aimed to evaluate T-joints with CHS braces and SHS chords and with chord face failure as the predicted failure mode. The analysis was made using a numerical model with finite elements developed in a commercial software, with variations of the chord thickness and the brace-to-chord ratio. Furthermore, the numerical results were compared with the analytical equation used for the design of T-joints from ABNT NBR 16239 [2].

2 Geometric properties, validity ranges and design

To evaluate the joint, geometric parameters, validity ranges and the current design formulations to verify the failure mode are necessary. The adopted parameters and their nomenclature are currently used in normative prescriptions, allowing the better understanding of the joint behavior.

The geometric parameters to evaluate the joint were shown in Figure 1, where the parameter β indicates the ratio between the brace and the chord widths and the parameter and 2γ indicate the chord cross section's slenderness.

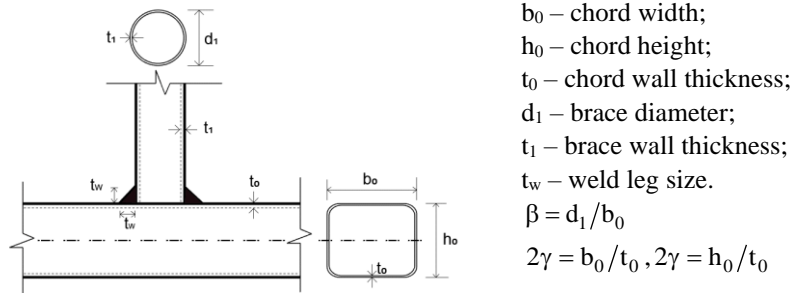


Figure 1. Geometric parameters.

The parameters used in the joint strength calculus for welded members have validity ranges that must be followed to obtain coherent results according to the equation recommended by the normative prescription. These conditions are related to the geometric and material properties of the joint members. Table 1 showed the geometric validity ranges for T-joints between circular hollow section braces and rectangular/square hollow section chords, according to ABNT NBR 16239 [2].

In T-joints with the parameter β lower or equal to 0.85, failure mode A – chord face failure – must be evaluated [6, 9]. The normative joint strengths were obtained with the ABNT NBR 16239 [2] equations, shown in Table 2. The ponderation factor (γ_{a1}) recommended is 1.10, but was not considered in this work.

Table 1. Validity conditions according to ABNT NBR 16239.

Condition	Axial load	Limits
SHS Brace	Compression	$d_1/t_1 \leq 0.05E/f_y$
SHS Chord	Tension	$h_0/t_0 \leq 35$
	Compression	$h_0/t_0 \leq \begin{cases} 36 \\ 1.45\sqrt{E/f_y} \end{cases}$

Table 2. Welded CHS-SHS T-joints resistance according to ABNT NBR 16239.

Failure mode A – T, Y and X joints $\beta \leq 0.85$	$N_{1,Rd} = \frac{k_n f_{y0} t_0^2}{1 - \beta} \frac{2.2\beta + 4.4\sqrt{1 - \beta} \left(\frac{\pi}{4} \right)}{\gamma_{a1}}$	$n = \frac{N_0}{N_{pl,0}} + \frac{M_0}{M_{el,0}}$	$n < 0, \quad k_n = 1.3 + \frac{0.4n}{\beta}$
			$n \geq 0, \quad k_n = 1.0$
$N_{1,Rd}$ – joint ultimate resistance; K_n – chord stress function; γ_{a1} – ponderation factor; β – brace-to-chord ratio; f_{y0} – chord yielding stress; n – non-dimensional chord stress ratio; N_0 – chord axial force design; M_0 – chord bending moment design; $N_{pl,0}$ – chord plastic axial force design; $M_{pl,0}$ – chord plastic moment capacity; $M_{el,0}$ – chord elastic moment capacity.			

3 Numerical analysis

3.1 Deformation limit criterion

A deformation limit criterion was used to determine the joint strength in the numerical analysis, which considered the displacements for the serviceability and ultimate strength limits. According to the deformation limit criterion by Lu et al. [7], the deformation (Δ) of 1% of the chord width (b_0) is the serviceability limit and the and a 3% deformation is the ultimate limit.

The joint resistance (N_{ult}) is determined according to the ratio between the deformation of the joint – chord face deformation – at 3% b_0 (N_3) and 1% b_0 (N_1) stages, as shown in Figure 2. If this ratio is lower than 1.5, N_{ult} is equal to N_3 ; if higher, N_{ult} must be equal to $1.5N_1$.

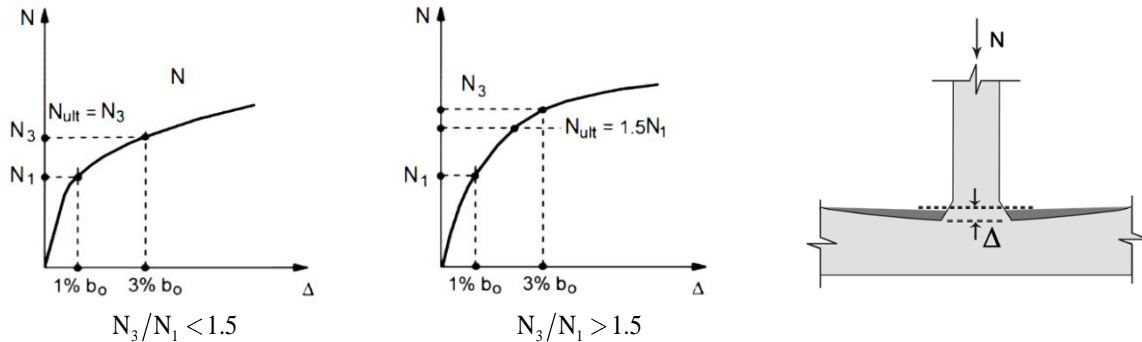


Figure 2. Deformation limit [8].

3.2 Parametric study

In the parametric study, 24 models were developed with chords of 1000 mm length and chord cross sections with 120mm x 120mm. Four different values of 2γ were analyzed: 30, 35, 40 and 45, in which the chord thicknesses varied according to this parameter.

The brace thickness adopted was equal to 6 mm, always higher than the chord thickness to avoid brace failure. The β values varied from 0.25 to 0.75 with 0.10 intervals. The brace diameter was defined according to the adopted β value. These dimensions were chosen to approach models with different chord cross sections' slenderness, with the specific geometric properties presented in Table 3.

The weld leg sized adopted was equal to 1.5 times the lower thickness value between the members of the connection, as recommended by ABNT NBR 16239 [2]. Therefore, the chord thickness governed the value of the weld leg size.

3.3 Material properties

The nominal properties of the materials used in the parametric study were presented in Table 4. Elastoplastic diagrams were adopted with nominal inclination for the materials of the braces and weld, represented in Figure 3. The elastoplastic diagram with hardening was adopted for the chords, represented in Figure 3 (b). The choices for these diagrams were based in studies by Pereira et al. [5] and Neto [10].

3.4 Numerical model

In the numerical structural analysis, a computational model was developed to represent the joint behavior. This model was created using the finite elements commercial software ANSYS [12].

In the definition of the finite element, the 3D modeling with solid elements was considered, as done in recent research of tubular joints by Vegte, Wardenier and Puthli [13], Pereira et al. [5] and Neto [10]. In this work, the finite element SOLID 185 was chosen, which has 8 nodes and three degrees of freedom by node, associated to the translations in the three axial directions.

In the mesh development, a refinement was made in the joint region (Figure 4), where lower size mesh was used to enable a more precise analysis of the failure mode predicted. The support condition with two fixed ends was simulated with node coupling in both ends, which degrees of freedom were restricted, not enabling translation nor rotation.

Furthermore, to avoid bending moments in the joint region, the chord was considered continuously simply supported, as experimentally studied by Lima et al. [14], who found that the numerical simulation of this condition led to adequate joint behavior results.

The analysis of the joint was static, with axial compression progressively applied to the braces through displacement control. The solution method chosen was the iterative Newton-Raphson.

Table 3. Geometric properties of the joints.

Model	$b_0=h_0$ (mm)	t_0 (mm)	d_1 (mm)	t_1 (mm)	β (d_1/b_0)	2γ (h_0/t_0)
1	120	4.0	30	6	0.25	30
2			42		0.35	
3			54		0.45	
4			66		0.55	
5			78		0.65	
6			90		0.75	
7	120	3.4	30	6	0.25	35
8			42		0.35	
9			54		0.45	
10			66		0.55	
11			78		0.65	
12			90		0.75	
13	120	3.0	30	6	0.25	40
14			42		0.35	
15			54		0.45	
16			66		0.55	
17			78		0.65	
18			90		0.75	
19	120	2.7	30	6	0.25	45
20			42		0.35	
21			54		0.45	
22			66		0.55	
23			78		0.65	
24			90		0.75	

Table 4. Material properties.

Elasticity modulus (GPa)		Yield tension (MPa)			
E	Tangent E_t	Weld E_w	Chord f_{y0}	Brace f_{y1}	Weld f_w
200	E/100	200	300	400	485

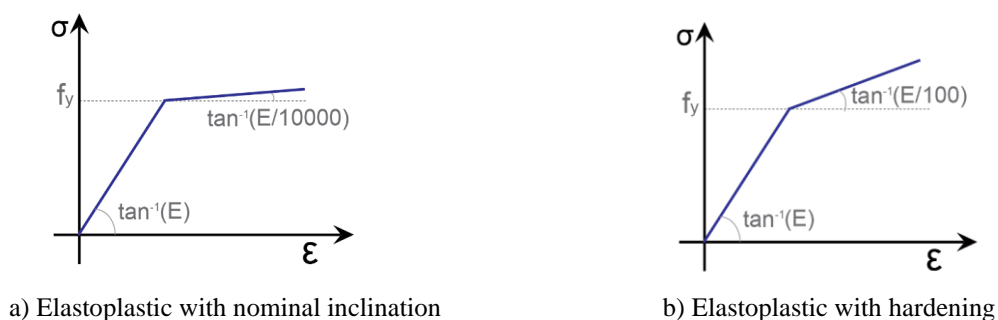


Figure 3. Stress versus strain steel diagrams [11].

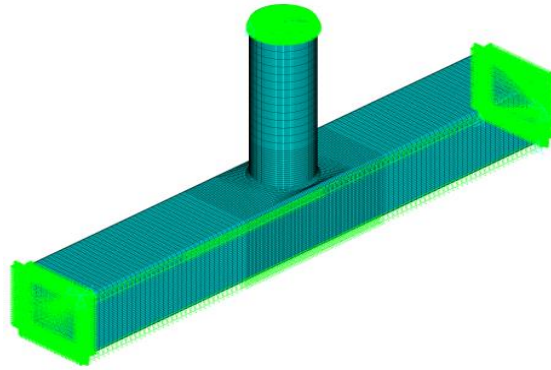


Figure 4. Finite elements mesh with boundary conditions applied.

4 Results

4.1 Failure mode and von Mises stress distribution

In Figure 5, the von Mises stress distributions were shown for two different models, with brace-to-chord ratios of 0.45 and 0.75. It was observed that there was a concentration of stresses in the joint region, specially in the encounter between braces and chord.

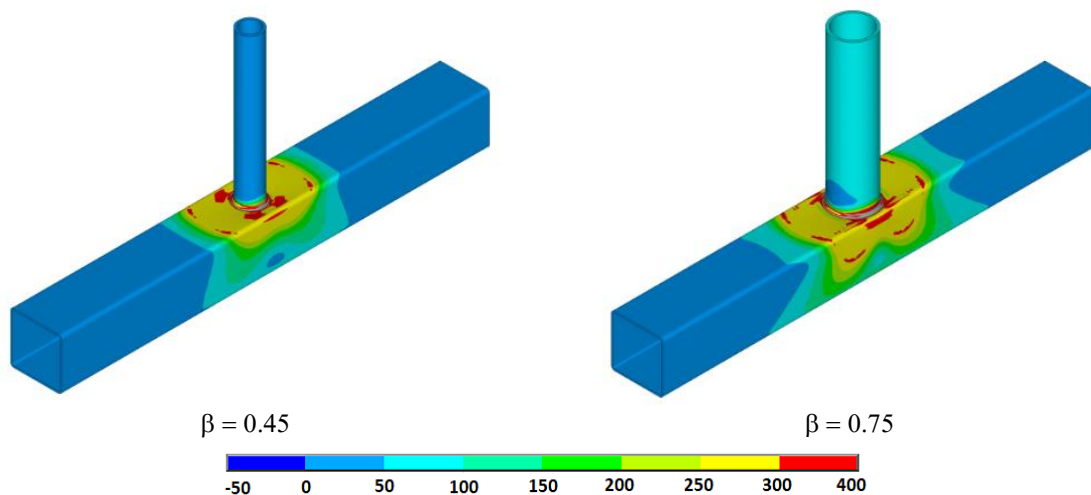


Figure 5. Von Mises stress distribution (MPa).

In Figure 6, it was observed that the ratio between lateral displacements (δ) and joint displacements (Δ) was always lower than 1.0, that is, the joint displacement in the chord upper face was always higher than the chord sidewall displacements, which characterizes chord face failure. It was also possible to infer that, with higher values of β , the δ/Δ ratio was also higher. This was also observable in Figure 5, in which the stress concentrations in the chord sidewalls were higher in the higher brace-to-chord (β) model.

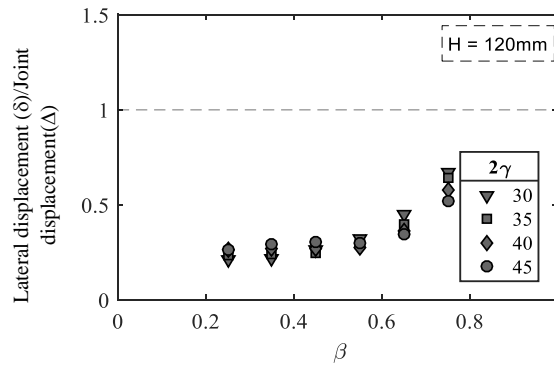


Figure 6. Lateral/superior displacements at the ultimate load stage.

4.2 Geometric parameters' influence in the joint resistance

To analyze the chord slenderness effect in the joint resistance, the chord thickness was varied, which caused the variation of the 2γ factor. Moreover, the variation of the parameter β was made, to enable the verification of the brace-to-chord ratio's influence in the joint behavior.

It was possible to observe that, in Figure 7, the ultimate joint strength was higher in cases of lower 2γ and higher β values, that is, higher thicknesses and higher brace diameters, respectively.

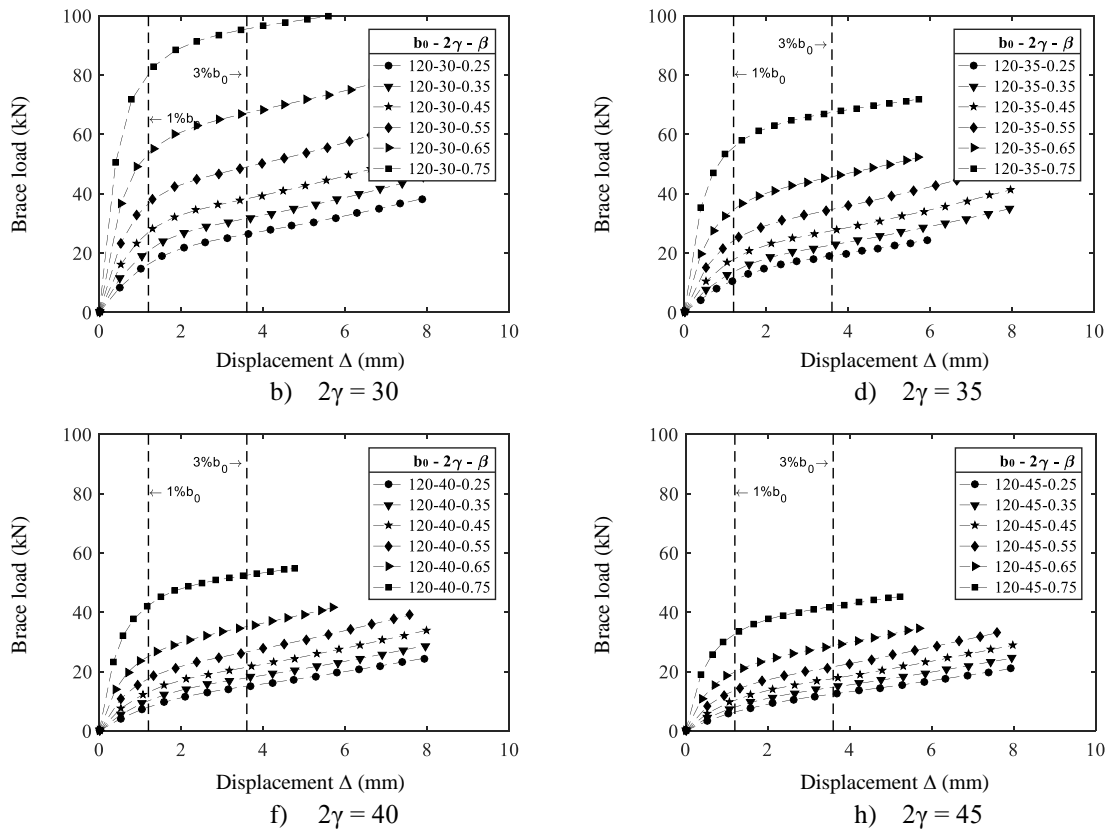


Figure 7. Load-displacement joint behavior.

5 Results comparison

In Table 5 the analytical ($N_{l,Rd}$) and numerical (N_{num}) values of joint strengths for each model were presented. It was observed that the numerical joint strengths of all models were higher than the analytical values, with a mean ratio between analytical by numerical strengths of 0.717.

Table 5. Results and comparison.

Model	2γ	β	$N_{1,Rd}$ (kN)	N_{num} (kN)	$N_{1,Rd}/N_{num}$	Model	2γ	β	$N_{1,Rd}$ (kN)	N_{num} (kN)	$N_{1,Rd}/N_{num}$
1*	30	0.25	19.9	24.3	0.82	13*	40	0.25	11.2	12.0	0.93
2*	30	0.35	22.8	31.1	0.73	14*	40	0.35	12.8	15.2	0.84
3	30	0.45	26.5	38.3	0.69	15*	40	0.45	14.9	19.6	0.76
4	30	0.55	31.7	49	0.65	16*	40	0.55	17.8	26.4	0.68
5	30	0.65	39.5	67.2	0.59	17*	40	0.65	22.2	35.2	0.63
6	30	0.75	52.8	95.5	0.55	18*	40	0.75	29.7	52.5	0.57
7*	35	0.25	14.4	16.2	0.89	19*	45	0.25	9.1	9.5	0.95
8*	35	0.35	16.4	20.5	0.80	20*	45	0.35	10.4	12.0	0.87
9	35	0.45	19.1	26.7	0.72	21*	45	0.45	12.1	15.4	0.78
10	35	0.55	22.9	34.7	0.66	22*	45	0.55	14.4	20.5	0.71
11	35	0.65	28.5	45.7	0.62	23*	45	0.65	18.0	28.8	0.63
12	35	0.75	38.1	67.4	0.57	24*	45	0.75	24.0	42.0	0.57

Mean $N_{1,Rd}/N_{num} = 0,717$.
*Outside the ABNT NBR 16239 validity ranges.

6 Conclusions

A study of T-joints between hollow steel sections with circular braces and square chords was performed, considering the variation of the chord wall thickness and the diameter of the braces. A numerical model was developed to analyze, through finite elements, the joint behavior and strength.

Chord face failure was the dominant failure mode in all cases studied, as it was expected for joints with the parameter β lower or equal to 0.85.

It was also observed that, for lower values of 2γ (higher thickness values) and higher β values, higher joint strength results were obtained.

The numerical results were compared with a normative analytical equation. It was verified that the general mean ratio between the joint strengths was 0.717.

Thus, the design of tubular T-joints with CHS braces and SHS chords, with the geometric parameters of the joints studied in this work, could be made with the current normative prescription equation, even though it is not recommended for joints with slender sections. However, the design for these joints was not precise, with high variations from the numerical results.

Acknowledgements. This work was made with the support from Coordenação de Aperfeiçoamento de Pessoal de Nível Superior – Brasil (CAPES) – Finance code 001, Fundação de Amparo à Pesquisa do Estado de Minas Gerais (FAPEMIG), Conselho Nacional de Desenvolvimento Científico e Tecnológico (CNPq), Universidade Federal de Ouro Preto (UFOP) and Instituto Federal de Minas Gerais (IFMG).

Authorship statement. The authors hereby confirm that they are the sole liable persons responsible for the authorship of this work, and that all material that has been herein included as part of the present paper is either the property (and authorship) of the authors or has the permission of the owners to be included here.

References

- [1] A. H. M. de Araújo, A. M. C. Sarmanho, E. de M. Batista, J. A. V. Requena, R. H. Fakury, and R. J. Pimenta, *Projeto de estruturas de edificações com perfis tubulares de aço*, 1st ed. Belo Horizonte: Editora Vallourec, 2016.
- [2] ABNT NBR 16239, *Projeto de estruturas de aço e de estruturas mistas de aço e concreto de edificações com perfis tubulares*, 1st ed. Rio de Janeiro: Associação Brasileira de Normas Técnicas, 2013.
- [3] D. J. R. Pereira, J. B. S. Neto, L. G. V. Alves, M. J. L. Guerra, G. V. Nunes, and A. M. C. Sarmanho, “Numerical study of CHS-SHS and CHS-RHS T-joints with chord web failure,” *Proc. XLI Ibero-Latin-American Congr. Comput. Methods Eng.*, 2020.
- [4] J. B. da S. Neto, D. J. R. Pereira, A. M. C. Sarmanho, M. J. L. Guerra, and L. G. V. Alves, “Ligações tubulares sujeitas à plastificação da face lateral do banzo,” in *VI CONENGE*, 2019, pp. 1663–1677.
- [5] D. J. R. Pereira, A. M. C. Sarmanho, G. V. Nunes, M. J. L. Guerra, and V. N. Alves, “Effect of fillet welds on T-joints with thin-walled chords,” *Proc. Inst. Civ. Eng. Struct. Build.*, vol. 172, no. 4, 2019, doi: 10.1680/jstbu.18.00043.
- [6] ISO 14346, *Static design procedure for welded hollow-section joints - Recommendations*. Geneva, Switzerland.

- Switzerland, Geneva: International Organization for Standardization, 2013.
- [7] L. H. Lu, G. D. de Winkel, Y. Yu, and J. Wardenier, "Deformation limit for the strength of hollow section joints," *Tubul. Struct.* VI, pp. 341–347, 1994.
- [8] X.-L. Zhao, "Deformation limit and ultimate strength of welded T-joints in cold-formed RHS sections," *J. Constr. Steel Res.*, vol. 53, no. 2, pp. 149–165, 2000, doi: 10.1016/S0143-974X(99)00063-2.
- [9] EN 1993-1-1, *Eurocode 3: Design of steel structures. Part 1-1: General rules and rules for buildings*. Brussels: CEN (European Committee for Standardization), 2005.
- [10] J. B. S. Neto, *Analysis numérica paramétrica de ligações do tipo T com carga no banzo*. Dissertação de Mestrado. Ouro Preto: Universidade Federal de Ouro Preto, 2020.
- [11] EN 1993-1-3, *Eurocode 3: Design of steel structures. Part 1-3: General rules - Supplementary rules for cold-formed members and sheeting*. Brussels: CEN (European Committee for Standardization), 2006.
- [12] ANSYS Inc., *ANSYS 12.1*. EUA: Swanson Analysis System, 2011.
- [13] G. J. Van Der Vegte, J. Wardenier, and R. S. Puthli, "FE analysis for welded hollow-section joints and bolted joints," *Proc. Inst. Civ. Eng. - Struct. Build.*, vol. 163, no. 6, pp. 427–437, 2010, doi: 10.1680/stbu.2010.163.6.427.
- [14] L. R. O. Lima, L. C. B. Guerreiro, P. C. G. da S. Vellasco, L. F. Costa-Neves, A. T. da Silva, and M. C. Rodrigues, "Experimental and numerical assessment of flange plate reinforcements on square hollow section T joints," *Thin-Walled Struct.*, vol. 131, pp. 595–605, Oct. 2018, doi: 10.1016/j.tws.2018.07.053.